

# Dynamical Quantum Phase Transitions in the Transverse Field Ising Model

M. Heyl

*Department of Physics, Arnold Sommerfeld Center for Theoretical Physics and Center for NanoScience,  
Ludwig-Maximilians-Universität München, Theresienstr. 37, 80333 Munich, Germany and  
Institut für Theoretische Physik, Technische Universität Dresden, 01062 Dresden, Germany*

A. Polkovnikov

*Department of Physics, Boston University, 590 Commonwealth Ave., Boston, MA 02215, USA*

S. Kehrein

*Department of Physics, Georg-August-Universität Göttingen,  
Friedrich-Hund-Platz 1, 37077 Göttingen, Germany*

A phase transition indicates a sudden change in the properties of a large system. For temperature-driven phase transitions this is related to non-analytic behavior of the free energy density at the critical temperature: The knowledge of the free energy density in one phase is insufficient to predict the properties of the other phase. In this paper we show that a close analogue of this behavior can occur in the real time evolution of quantum systems, namely non-analytic behavior at a critical time. We denote such behavior a *dynamical phase transition* and explore its properties in the transverse field Ising model. Specifically, we show that the equilibrium quantum phase transition and the dynamical phase transition in this model are intimately related.

Phase transitions are one of the most remarkable phenomena occurring in many-particle systems. At a phase transition a system undergoes a non-analytic change of its properties, for example the density at a temperature driven liquid-gas transition, or the magnetization at a paramagnet-ferromagnet transition. What makes the theory of such equilibrium phase transitions particularly fascinating is the observation that a perfectly well-behaved microscopic Hamiltonian without any singular interactions can lead to non-analytic behavior in the thermodynamic limit of the many-particle system. In fact, the occurrence of equilibrium phase transitions was initially a puzzling problem because one can easily verify no go theorems for finite systems, therefore the thermodynamic limit is essential [1].

Today the theory of equilibrium phase transitions is well established, especially for classical systems undergoing continuous transitions, where the powerful tool of renormalization theory bridges the gap from microscopic Hamiltonian to universal macroscopic behavior. On the other hand, the behavior of non-equilibrium quantum many-body systems is by far less well understood. Recent experimental advances have triggered a lot of activity in this field [3], like the experiments on the real time evolution of essentially closed quantum systems in cold atomic gases [3, 4]. The experimental setup is typically a quantum quench, that is a sudden change of some parameter in the Hamiltonian. Therefore the system is initially prepared in a non-thermal superposition of the eigenstates of the Hamiltonian which drives its time evolution.

From a formal point of view, there is a very suggestive similarity between the canonical partition function of an equilibrium system

$$Z(\beta) = \text{Tr} e^{-\beta H} \quad (1)$$

and the overlap amplitude of some time-evolved initial quantum state  $|\Psi_i\rangle$  with itself

$$G(t) = \langle \Psi_i | e^{-iHt} | \Psi_i \rangle \quad (2)$$

This leads to the question whether some analogue of temperature ( $\beta$ )-driven equilibrium phase transitions in (1) exists in real time evolution problems. In the theory of equilibrium phase transitions it is well established that the breakdown of the high-temperature (small  $\beta$ ) expansion indicates a temperature-driven phase transition. Likewise, we propose the term *dynamical phase transition* for non-analytic behavior in time, that is the breakdown of a short time expansion in the thermodynamic limit at a critical time. In this paper we study this notion of dynamical phase transition in the one dimensional transverse field Ising model, which serves as a paradigm for one dimensional quantum phase transitions [5]. It can be solved exactly, which permits us to establish the existence of dynamical phase transitions that are intimately related to the equilibrium quantum phase transition in this model.

Our key quantity of interest is the boundary partition function

$$Z(z) = \langle \Psi_i | e^{-zH} | \Psi_i \rangle \quad (3)$$

in the complex plane  $z \in \mathbb{C}$ . For imaginary  $z = it$  this just describes the overlap amplitude (2). For real  $z = R$  it can be interpreted as the partition function of the field theory described by  $H$  with boundaries described by boundary states  $|\Psi_i\rangle$  separated by  $R$  [6]. In the thermodynamic limit one defines the free energy density (apart from a different normalization)

$$f(z) = - \lim_{N \rightarrow \infty} \frac{1}{N} \ln Z(z) \quad (4)$$

where  $N$  is the number of degrees of freedom. Now subject to a few technical conditions [1] one can show that for finite  $N$  the partition function (3) is an entire function of  $z$  since inserting an eigenbasis of  $H$  yields sums of terms  $e^{-zE_j}$ , which are entire functions of  $z$ . According to the Weierstrass factorization theorem [7] an entire function with zeroes  $z_j \in \mathbb{C}$  can be written as

$$Z(z) = e^{h(z)} \prod_j \left(1 - \frac{z}{z_j}\right) \quad (5)$$

with an entire function  $h(z)$ . Thus

$$f(z) = - \lim_{N \rightarrow \infty} \frac{1}{N} \left[ h(z) + \sum_j \ln \left(1 - \frac{z}{z_j}\right) \right] \quad (6)$$

and the non-analytic part of the free energy density is solely determined by the zeroes  $z_j$ . A similar observation was originally made by M. E. Fisher [1], who pointed out that the partition function (1) is an entire function in the complex temperature plane. This observation is analogous to the Lee-Yang analysis of equilibrium phase transitions in the complex magnetic field plane [8]. For example in the 2d Ising model the Fisher zeroes in the complex temperature plane approach the real axis at the critical temperature  $z = \beta_c$  in the thermodynamic limit, indicating its phase transition [9].

We now work out these analytic properties explicitly for the one dimensional transverse field Ising model (with periodic boundary conditions)

$$H(g) = -\frac{1}{2} \sum_{i=1}^{N-1} \sigma_i^z \sigma_{i+1}^z + \frac{g}{2} \sum_{i=1}^N \sigma_i^x \quad (7)$$

For magnetic field  $g < 1$  the system is ferromagnetically ordered at zero temperature, and a paramagnet for  $g > 1$  [5]. These two phases are separated by a quantum critical point at  $g = g_c = 1$ . The Hamiltonian (7) can be mapped to a quadratic fermionic model [10–12]

$$H(g) = -\frac{1}{2} \sum_{i=1}^{N-1} \left( c_i^\dagger c_{i+1} + c_i^\dagger c_{i+1}^\dagger + \text{h.c.} \right) + g \sum_{i=1}^N c_i^\dagger c_i \quad (8)$$

Diagonalization yields the dispersion relation  $\epsilon_k(g) = \sqrt{(g - \cos k)^2 + \sin^2 k}$ .

In a quantum quench experiment the system is prepared in the ground state for parameter  $g_0$ ,  $|\Psi_i\rangle = |\Psi_{GS}(g_0)\rangle$ , while its time evolution is driven with a Hamiltonian  $H(g_1)$  with a different parameter  $g_1$ . In the sequel we will first analyze quench experiments in the setting of the fermionic model (8). A subtle difference occurs when thinking in terms of the spin model (7) since in the ferromagnetic phase the ground state of the spin model is twofold degenerate, while the fermionic model always has a unique ground state. We will say more about this

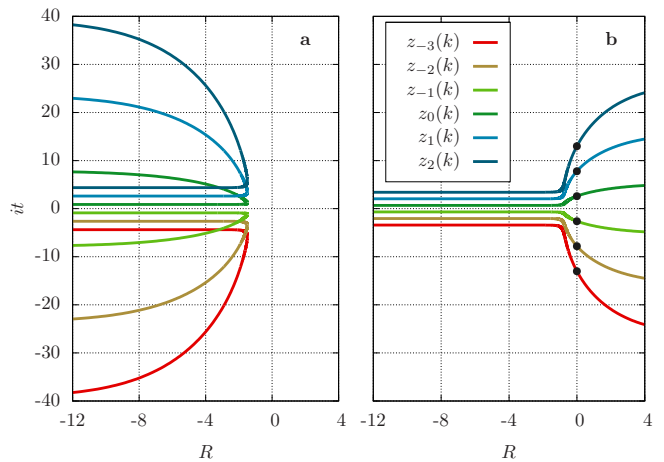


Figure 1: Lines of Fisher zeroes for a quench within the same phase  $g_0 = 0.4 \rightarrow g_1 = 0.8$  (left) and across the quantum critical point  $g_0 = 0.4 \rightarrow g_1 = 1.3$  (right). Notice that the Fisher zeroes cut the time axis for the quench across the quantum critical point, giving rise to non-analytic behavior at  $t_n^*$  (the times  $t_n^*$  are marked with dots in the plot).

later. Taking the ground state of the fermionic model in Eq. (8) as the initial state  $|\Psi_i\rangle$  the free energy density (4) describing this sudden quench  $g_0 \rightarrow g_1$  can be calculated analytically [4] yielding

$$f_{g_0, g_1}(z) = - \int_0^\pi \frac{dk}{2\pi} \ln \left( \cos^2 \phi_k + \sin^2 \phi_k e^{-2z\epsilon_k(g_1)} \right) \quad (9)$$

Here  $\phi_k = \theta_k(g_0) - \theta_k(g_1)$ , and  $\tan(2\theta_k(g)) \stackrel{\text{def}}{=} \sin k / (g - \cos k)$ ,  $\theta_k(g) \in [0, \pi/2]$ . In (9) we have ignored an uninteresting additive contribution  $z E_{GS}(g_1)/N$  that depends on the ground state energy of  $H(g_1)$ .

In the thermodynamic limit the zeroes of the partition function in the complex plane coalesce to a family of lines labeled by a number  $n \in \mathbb{Z}$

$$z_n(k) = \frac{1}{2\epsilon_k(g_1)} \left( \ln \tan^2 \phi_k + i\pi(2n + 1) \right) \quad (10)$$

The limiting infrared and ultraviolet behavior of the Boboliubov angles

$$\phi_{k=0} = \begin{cases} 0 & \text{quench in same phase} \\ \pi/4 & \text{quench to/from quantum critical point} \\ \pi/2 & \text{quench across quantum critical point} \end{cases} \\ \phi_{k=\pi} = 0 \quad (11)$$

immediately shows that the lines of Fisher zeroes cut the time axis for a quench across the quantum critical point (Fig. 1) since then  $\lim_{k \rightarrow 0} \text{Re } z_n(k) = \infty$ ,  $\lim_{k \rightarrow \pi} \text{Re } z_n(k) = -\infty$ . In fact, the limiting behavior (11) remains unchanged for general ramping protocols [14].

The free energy density (4) is just the rate function of the return amplitude  $G(t) = \exp[-N f(it)]$ . Likewise for the return probability (Loschmidt echo)  $L(t) \stackrel{\text{def}}{=} |G(t)|^2 = \exp(-N l(t))$  one has  $l(t) = f(it) + f(-it)$ . The behavior of the Fisher zeroes for quenches across the quantum critical point therefore translates into non-analytic behavior of the rate functions for return amplitude and probability at certain times  $t_n^*$ . For sudden quenches one can work out these times easily

$$t_n^* = t^* \left( n + \frac{1}{2} \right), \quad n = 0, 1, 2, \dots \quad (12)$$

with  $t^* = \pi/\epsilon_{k^*}(g_1)$  and  $k^*$  determined by  $\cos k^* = (1 + g_0 g_1)/(g_0 + g_1)$ . We conclude that for any quench across the quantum critical point the short time expansion for the rate function of the return amplitude and probability breaks down in the thermodynamic limit, analogous to the breakdown of the high-temperature expansion at an equilibrium phase transition. In fact, the non-analytic behavior of  $l(t)$  at the times  $t_n$  has already been derived by Pollmann et al. [15] for slow ramping across the quantum critical point. For a slow ramping protocol  $\epsilon_{k^*}(g_1)$  becomes the mass gap  $m(g_1) = |g_1 - 1|$  of the final Hamiltonian, but in general it is a new energy scale generated by the quench and depending on the ramping protocol. In the universal limit for a quench across but very close to the quantum critical point,  $g_1 = 1 + \delta$ ,  $|\delta| \ll 1$  and fixed  $g_0$ , one finds  $\epsilon_{k^*}(g_1)/m(g_1) \propto 1/\sqrt{|\delta|}$ . Hence in this limit the non-equilibrium energy scale  $\epsilon_{k^*}$  becomes very different from the mass gap, which is the only equilibrium energy scale of the final Hamiltonian.

The interpretation of the mode  $k^*$  follows from the observation  $n(k^*) = 1/2$ , where  $n(k)$  is the occupation of the excited state in the momentum  $k$ -mode in the eigenbasis of the final Hamiltonian  $H_f(g_1)$ . Modes  $k > k^*$  have thermal occupation  $n(k) < 1/2$ , while modes  $k < k^*$  have inverted population  $n(k) > 1/2$  and therefore formally negative effective temperature. The mode  $k^*$  corresponds to infinite temperature. In fact, the existence of this infinite temperature mode and thus of the Fisher zeroes cutting the time axis periodically is guaranteed for arbitrary ramping protocols across the quantum critical point. For example, for slow ramping across the quantum critical point the existence of this mode and the negative temperature region in relation to spatial correlations was discussed in Ref. [16].

One measurable quantity in which the non-analytic behavior generated by the Fisher zeroes appears naturally is the work distribution function of a double quench experiment: We prepare the system in the ground state of  $H(g_0)$ , then quench to  $H(g_1)$  at time  $t = 0$ , and then quench back to  $H(g_0)$  at time  $t$ . The amount of work  $W$

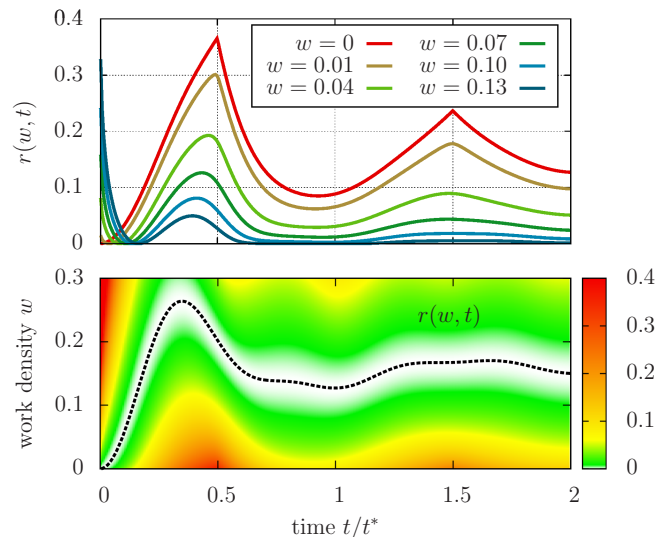


Figure 2: The bottom plot shows the work distribution function  $r(w, t)$  for a double quench across the quantum critical point ( $g_0 = 0.5$ ,  $g_1 = 2.0$ ). The dashed line depicts the expectation value of the performed work,  $r(w, t) = 0$ . The top plot shows various cuts for fixed values of the work density  $w$ . The line  $w = 0$  is just the Loschmidt echo: Its non-analytic behavior at  $t_n^*$  becomes smooth for  $w > 0$ , but traces of the non-analytic behavior extend into the work density plane. In this respect work density plays a similar role to temperature in the phase diagram of an equilibrium quantum phase transition.

performed follows from the distribution function

$$P(W, t) = \sum_j \delta(W - (E_j - E_{GS}(g_0))) |\langle E_j | \Psi_i(t) \rangle|^2 \quad (13)$$

where the sum runs over all eigenstates  $|E_j\rangle$  of the initial Hamiltonian  $H(g_0)$ . It obeys a large deviation form  $P(W, t) \sim e^{-N r(w, t)}$  with a rate function  $r(w, t) \geq 0$  depending on the work density  $w = W/N$ . In the thermodynamic limit one can derive an exact result for  $r(w, t)$ : According to the Gärtner-Ellis theorem [17] it is just the Legendre transform

$$-r(w, t) = \inf_{R \in \mathbb{R}} (wR - c(R, t)) \quad (14)$$

where

$$c(R, t) = - \int_0^\pi \frac{dk}{2\pi} \ln \left( 1 + \sin^2(2\phi_k) \sin^2(\epsilon_k(g_1)t) \right) \times (e^{-2\epsilon_k(g_0)R} - 1) \quad (15)$$

is the rate function for the cumulant generating function of the work distribution function,  $C(R, t) = \int dW P(W, t) e^{-RW} = e^{-N c(R, t)}$ . In Fig. Fig. 2 we show  $r(w, t)$  for a quench across the quantum critical point. For  $w = 0$  it just gives the return probability to the ground state,  $r(w = 0, t) = l(t)$ , therefore the non-

analytic behavior at the Fisher zeroes shows up as non-analytic behavior in the work distribution function. However, from Fig. 2 one can see that these non-analyticities at  $w = 0$  also dominate the behavior for  $w > 0$  at  $t_n^*$ , corresponding to more likely values of the performed work. The suggestive similarity to the phase diagram of a quantum critical point, with temperature being replaced by the work density  $w$ , motivates us to call this behavior dynamical *quantum* phase transitions. Notice that experimentally the work density can be lowered by *post-selection* [13].

So far we have analyzed the quench dynamics in terms of the fermionic model (8). When thinking in terms of the transverse field Ising model (7), all results carry over for quenches starting in the paramagnetic phase since then the spin ground state is unique. Specifically, one finds the non-analytic behavior in the Loschmidt echo *and* the work distribution function for quenches from the paramagnetic to the ferromagnetic phase. For quenches originating in the ferromagnetic phase, the Loschmidt echo calculated above corresponds to working in the Neveu-Schwarz sector [21], which amounts to an unphysical superposition of spin up and spin down ground states in the spin language. However, looking at the experimentally relevant quantity work distribution function, one derives the same result in the thermodynamic limit as above when starting from either of the two degenerate ferromagnetic ground states. Specifically, one obtains the non-analytic behavior in  $P(w = 0, t)$  at the critical times (12) for quenches from the ferromagnetic to the paramagnetic phase [13].

Interestingly, the non-equilibrium time scale (12) also plays a role in the dynamics of a local observable after the quench. We have calculated the longitudinal magnetization by numerical evaluation of Pfaffians [1]. For quenches within the ordered phase it is known analytically [19, 20] that the order parameter decays exponentially as a function of time, which is expected since in equilibrium one only finds long range order at zero temperature ( $g < 1$ ). For a quench across the quantum critical point an additional oscillatory behavior is superimposed on this exponential decay, see Fig. 3. Notice that the behavior of the magnetization remains perfectly analytic, but the period of its oscillations agrees exactly (within numerical accuracy) with the period  $t^*$  of Fisher times. A conjecture consistent with our observation was also formulated in Ref. [21]. A better understanding of this observation will be the topic of future work. At low energies the oscillatory decay transforms into real-time nonanalyticities at the Fisher times using the concept of post-selection allowing to observe the dynamical phase transitions in local observables [13].

Summing up, we have shown that ramping across the quantum critical point of the transverse field Ising

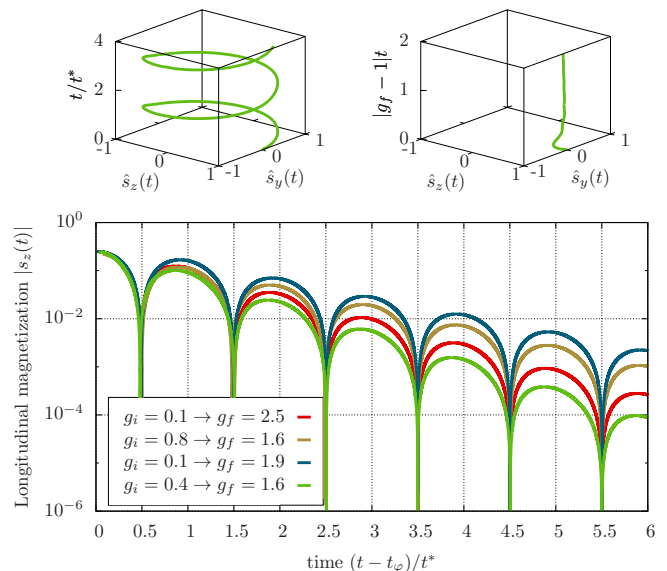


Figure 3: Dynamics of the magnetization after the quench. The bottom plot shows the longitudinal magnetization for various quenches across the quantum critical point. The time axis is shifted by a fit parameter  $t_\varphi$  and one can see that the period of the oscillations is the time scale  $t^*$  (12). The upper plots show the magnetization dynamics in the  $y-z$ -plane for a quench across the quantum critical point  $g_0 = 0.3 \rightarrow g_1 = 1.4$  (left) and a quench in the ordered phase  $g_0 = 0.3 \rightarrow g_1 = 0.8$  (right). For better visibility the magnetization is normalized to unit length:  $\hat{s}_{y,z}(t) \stackrel{\text{def}}{=} s_{y,z}(t)/\sqrt{s_y^2(t) + s_z^2(t)}$ . Notice the Larmor precession for the quench across the quantum critical point, while the dynamics for the quench in the ordered phase is asymptotically just an exponential decay [19].

model generates periodic non-analytic behavior at certain times  $t_n^*$ . This breakdown of the short time expansion is reminiscent of the breakdown of a high temperature expansion for the free energy at an equilibrium phase transition. We have therefore denoted this behavior *dynamical phase transition*. Notice that there are other related but not identical notions of dynamical phase transitions, for example a sudden change of the dynamical behavior of an observable as a function of some control parameter [22, 23], or qualitative changes in the ensemble of trajectories, as a function of the conjugate field of a dynamical order parameter [24].

For quenches within the same phase (including to/from the quantum critical point) the lines of Fisher zeroes lie in the negative half plane,  $\text{Re } z_j(k) \leq 0$  (Fig. 1). Hence the knowledge of the equilibrium free energy  $f(R)$  on the positive real axis completely determines the time evolution by a simple Wick rotation. This is no longer true for a quench/ramping protocol across the quantum critical point since then the lines of Fisher zeroes cut the complex plane into disconnected stripes, Fig. 1: Knowing  $f(R)$  for  $R \geq 0$  does not determine the time evolution for  $t > t_0^*$ . In this sense non-equilibrium time evolution is no longer

described by equilibrium properties.

The authors thank L. D'Alessio, M. Kolodrubetz and D. Huse for valuable discussions. The authors also acknowledge the support of the Deutsche Forschungsgemeinschaft via SFB-TR 12, the German Excellence Initiative via the Nanosystems Initiative Munich (M.H. and S.K.), the NSF under grants DMR-0907039, PHY11-25915, the AFOSR under grant FA9550-10-1-0110, the Sloan and Simons Foundations (A.P.). S.K. thanks the Boston University visitors program, A.P. and S.K. thank the Kavli Institute for Theoretical Physics at UCSB for their hospitality and NSF PHY11-25915.

- 
- [1] M. E. Fisher, in: *Boulder Lectures in Theoretical Physics, Vol. 7* (University of Colorado, Boulder, 1965).
- [2] A. Polkovnikov, K. Sengupta, A. Silva, and M. Vengalattore, *Rev. Mod. Phys.* **83**, 863 (2011).
- [3] M. Greiner, O. Mandel, T. Esslinger, T. Hänsch, and I. Bloch, *Nature* **419**, 51 (2002).
- [4] T. Kinoshita, T. Wenger, and D. Weiss, *Nature* **440**, 900 (2006).
- [5] S. Sachdev, *Quantum Phase Transitions* (Cambridge University Press, Cambridge, 2011).
- [6] A. LeClair, G. Mussardo, H. Saleur, and S. Skorik, *Nucl. Phys. B* **453**, 581 (1995).
- [7] J. B. Conway, *Functions of One Complex Variable* (Springer, New York, 1995).
- [8] C. Yang and T. Lee, *Phys. Rev.* **87**, 404 (1952).
- [9] W. van Saarloos and D. Kurtze, *J. Phys. A* **17**, 1301 (1984).
- [10] E. Lieb, T. Schultz, and D. Mattis, *Ann. Phys.* **16**, 407 (1961).
- [11] P. Pfeuty, *Ann. Phys.* **57**, 79 (1970).
- [12] E. Barouch, B. McCoy, and M. Dresden, *Phys. Rev. A* **2**, 1075 (1970).
- [13] See Supplementary material for details about Loschmidt echos for symmetry broken initial states and post-selection.
- [14] For a general ramping protocol  $g(t)$  with  $g(t = 0) = g_0, g(t = \tau) = g_1$  we define  $|\Psi_i\rangle = |\psi(\tau)\rangle$  and  $|\psi(t)\rangle$  is the solution of the Schroedinger equation:  $i \partial_t |\psi(t)\rangle = H(g(t)) |\psi(t)\rangle$ ,  $|\psi(t = 0)\rangle = |\Psi_{GS}(g_0)\rangle$
- [15] F. Pollmann, S. Mukerjee, A. Green, and J. Moore, *Phys. Rev. E* **81**, 020101 (R) (2010).
- [16] M. Kolodrubetz, B. Clark, and D. Huse, *Phys. Rev. Lett.* **109**, 015701 (2012).
- [17] H. Touchette, *Phys. Rep.* **478**, 1 (2009).
- [18] E. Barouch and B. McCoy, *Phys. Rev. A* **3**, 786 (1971).
- [19] P. Calabrese, T. Essler, and M. Fagotti, *Phys. Rev. Lett.* **106**, 227203 (2011).
- [20] D. Schuricht and F. Essler, *J. Stat. Mech.* P04017 (2012).
- [21] P. Calabrese, F. Essler, and M. Fagotti, *J. Stat. Mech.* P07016 (2012).
- [22] M. Eckstein, M. Kollar, and P. Werner, *Phys. Rev. Lett.* **103**, 056403 (2009).
- [23] B. Sciolla and G. Biroli, *J. Stat. Mech.* **11**, P11003 (2011).
- [24] J. Garrahan and I. Lesanovsky, *Phys. Rev. Lett.* **104**, 160601 (2010).

- [25] B. McCoy, E. Barouch, and D. Abraham, *Phys. Rev. A* **4**, 2331 (1971).

### Loschmidt matrix

For Hamiltonians with symmetry-broken ground states the definition of the return amplitude in Eq. (2) in the main text shares an ambiguity: there is not a unique ground state and therefore initial state  $|\Psi_i\rangle$  for the nonequilibrium time evolution. Moreover, the return amplitude turns out to depend crucially on the precise choice of initial state in the degenerate ground state manifold for quenches across the quantum critical point in the Ising model for  $g_0 < 1$  as will be shown in detail below. This is of particular importance because the ground state  $|\Psi_{GS}(g_0)\rangle$  of the fermionic version of the Ising chain in Eq. (8) is not identical to one of the symmetry broken ferromagnetic ground states but rather to some superposition. The aim of this supplementary material is to demonstrate that, although the return amplitude depends on the precise choice of initial state, the experimentally relevant quantity, i.e., the work distribution of the double quench in Eq. (13), does not. As a consequence, the free energy density of the fermionic model in Eq. (9) is the relevant quantity although  $|\Psi_{GS}(g_0)\rangle$  is not the initial state of the quantum quench protocol.

In case of symmetry broken ground states we propose the following generalization for the return amplitude that we will term the Loschmidt matrix:

$$\mathcal{L}(t) = \begin{pmatrix} \langle \Psi_1 | e^{-iH_f t} | \Psi_1 \rangle & \langle \Psi_1 | e^{-iH_f t} | \Psi_2 \rangle \\ \langle \Psi_2 | e^{-iH_f t} | \Psi_1 \rangle & \langle \Psi_2 | e^{-iH_f t} | \Psi_2 \rangle \end{pmatrix} \quad (16)$$

shown here for the case of two symmetry broken ground states  $|\Psi_1\rangle$  and  $|\Psi_2\rangle$ . The generalization to more than two states is straightforward. This matrix depends on the particular choice of the basis wave functions  $|\Psi_1\rangle$  and  $|\Psi_2\rangle$  in the degenerate ground state manifold. From a physical point of view, there is, however, a unique choice: the symmetry broken ground states. In case of vanishing transverse magnetic field in the Ising model this will be the fully polarized states  $|\Psi_1\rangle = |\uparrow \dots \uparrow\rangle$  or  $|\Psi_2\rangle = |\downarrow \dots \downarrow\rangle$ , for example.

Note that neither  $|\Psi_1\rangle$  nor  $|\Psi_2\rangle$  are the ground state  $|\Psi_{GS}(g_0)\rangle$  of the fermionized model in Eq. (8) in the ferromagnetic phase. This can be seen directly by noticing that  $|\Psi_{GS}(g_0)\rangle$  carries no magnetization  $\langle \Psi_{GS}(g_0) | \sigma_i^z | \Psi_{GS}(g_0) \rangle = 0$ . Concluding  $|\Psi_{GS}(g_0)\rangle$  rather is a superposition of  $|\Psi_1\rangle$  and  $|\Psi_2\rangle$ . Fortunately, for most of the quantities considered in the literature such as the spin-spin correlation function  $\sigma_i^z \sigma_m^z$  this makes no difference. This actually allows for the calculation of the absolute value of the magnetization even in the fermionic language using the cluster decomposition  $\langle \Psi_{1/2}(g_0) | \sigma_l^z | \Psi_{1/2}(g_0) \rangle^2 =$

$\lim_{m \rightarrow \infty} \langle \Psi_{GS}(g_0) | \sigma_{l+m}^z \sigma_l^z | \Psi_{GS}(g_0) \rangle$  [1]. Some quantities, however, such as the magnetization itself and the return amplitudes (as will be shown in detail below) the precise choice of the initial state can be crucial.

In the following we demonstrate the dependence of the return amplitude on the initial state for quenches from the ferromagnetic to the paramagnetic phase. We illustrate this subtle behavior for the particular example of a quench from  $g_0 = 0$  to  $g_1 \gg 1$ . This case can be solved exactly and directly for the initial spin Hamiltonian in Eq. (7) without using the mapping onto the fermionic language. For such a quench the Loschmidt matrix is given by

$$\mathcal{L}(t) = \begin{pmatrix} e^{-Nf_{11}(t)} & e^{-Nf_{12}(t)} \\ e^{-Nf_{21}(t)} & e^{-Nf_{22}(t)} \end{pmatrix} \quad (17)$$

with

$$\begin{aligned} f_{11}(t) &= f_{22}(t) = \log(|\cos(g_1 t/2)|) \\ f_{12}(t) &= f_{21}(t) = \log(|\sin(g_1 t/2)|) \end{aligned} \quad (18)$$

Here, we have ignored imaginary parts as they are not important for the discussion below. Note the large deviation scaling of the Loschmidt matrix elements that are exponentially suppressed with system size  $N$ . If  $\text{Re}[f_{11}(t)] > \text{Re}[f_{12}(t)]$  the Loschmidt matrix is effectively diagonal in the thermodynamic limit  $N \gg 1$  whereas in the opposite case it only carries off-diagonal entries. For small times the diagonal elements typically dominate. But for sufficiently large times the off-diagonal components can build up indicating the possibility of transitions between the two different symmetry broken ground states. As we explain below this switching underlies the dynamical phase transition we are discussing.

The return amplitude  $G(t)$  for the ground state  $|\Psi_{GS}(g_0)\rangle$  of the fermionic model (which is a superposition of  $|\Psi_1\rangle$  and  $|\Psi_2\rangle$ ) and thus the free energy density  $f(t)$  in Eq. (9) is given by

$$\begin{aligned} G(t) &= e^{-Nf(t)} = \langle \Psi_{GS}(g_0) | e^{-itH_F} | \Psi_{GS}(g_0) \rangle = \\ &= e^{-Nf_{11}(t)} + e^{-Nf_{12}(t)}. \end{aligned} \quad (19)$$

Due to the large deviation scaling of the Loschmidt matrix elements the precise coefficients of the superposition are subleading and therefore do not appear in this equation. This is the case as long as no coefficient is exactly zero or scales exponentially with system size. The diagonal elements of the free energy densities  $f_{11}(t) = f_{22}(t)$  are analytic at the Fisher times  $t_n^* = t^*(n + 1/2)$  with  $t^* = \pi/g_1$ . Instead, they show logarithmic singularities at times  $t = 2t^*(n + 1/2) \neq t_m^*$  for all  $n, m \in \mathbb{Z}$ . However, at the Fisher times  $\text{Re}[f_{11}(t_n^*)] = \text{Re}[f_{12}(t_n^*)]$ , i.e.,  $\sin(|g_1 t_n^*/2|) = \cos(|g_1 t_n^*/2|)$ , and both the diagonal and off-diagonal contributions become identical. This signals a critical point where the dominant contribution to the

Loschmidt matrix changes from the diagonal to the off-diagonal sector and vice versa. For the free energy density  $f(t)$  this implies the following result

$$f(t) = \begin{cases} f_{11}(t) & , \text{ if } t_{2n-1}^* < t < t_{2n}^* \\ f_{12}(t) & , \text{ if } t_{2n}^* < t < t_{2n+1}^* \end{cases}, n \in \mathbb{Z}. \quad (20)$$

Concluding, the singularity in  $f(t)$  is in fact not because the diagonal free energies are singular but rather because at the Fisher times  $t_n^*$  the free energy switches between  $f_{11}(t)$  and  $f_{12}(t)$ . Physically it implies that at the first Fisher time, for example, the return probability becomes dominated by the transition to a different magnetization sector.

Although the precise choice of initial state can be crucial for the return amplitude, in the following we demonstrate that the work distribution function  $P(W, t)$  of a double quench defined in Eq. (13) is independent of all these subtleties. This is important as  $P(W, t)$  is the experimentally measurable and therefore relevant quantity. In the zero work limit one obtains

$$\lim_{W \rightarrow 0} P(W, t) = |\langle \Psi_1 | \Psi_0(t) \rangle|^2 + |\langle \Psi_2 | \Psi_0(t) \rangle|^2 \quad (21)$$

with  $|\Psi_0(t)\rangle = e^{-iH_f t} |\Psi_0\rangle$  the time evolved initial state  $|\Psi_0\rangle$ . Irrespective of the precise choice of  $|\Psi_0\rangle$  in the ground state manifold (could also be one of the symmetry broken ground states)  $P(W \rightarrow 0, t)$  always contains contributions from both magnetization sectors:

$$\begin{aligned} P(W \rightarrow 0, t) &= e^{-2N\text{Re}[f_{11}(t)]} + e^{-2N\text{Re}[f_{12}(t)]} = \\ &= e^{-2N\text{Re}[f(t)]}. \end{aligned} \quad (22)$$

For the derivation of this equality the large deviation scaling of the probabilities is essentially important. Although  $|\Psi_{GS}(g_0)\rangle$  is not the correct initial state for the quantum quench (it is not one of the symmetry broken ground states) its associated return amplitude with rate function  $f(t)$  fully determines the experimentally relevant work distribution function:

$$P(W \rightarrow 0) = |\langle \Psi_{GS}(g_0) | e^{-iH_f t} | \Psi_{GS}(g_0) \rangle|^2. \quad (23)$$

The analysis in this supplementary material has illustrated the dependence of the return amplitude on the choice of initial state for the extreme quench from  $g_0 = 0$  to  $g_1 \gg 1$ . Although the return amplitude depends on this choice, the work distribution for a double quench does not.

It is possible to also include  $1/g_1$  corrections in the calculation of the return amplitude using the original spin language for large but finite magnetic fields  $g_1$ . It turns out that this improved treatment fully supports the conclusions drawn above. This analysis, however, is beyond the scope of this supplementary material and will be presented elsewhere.

### Postselection of observables

One route towards the experimental observation of the dynamical phase transitions in local observables is the idea of post-selection. Let us consider the double-quench experiment as discussed in the main text but with a slightly additional twist. Namely we assume that the system is prepared in the ground state of the initial Hamiltonian (actually the initial state can be arbitrary) then the Hamiltonian of the system is quenched to the final Hamiltonian  $H_f$  for the time  $t$  and then quenched back to the initial Hamiltonian  $H_i$ . After that we allow the system to relax to the diagonal ensemble [2], which using a different language also means measuring the energy of the system [3]. In the resulting diagonal state we measure the expectation value of an arbitrary observable  $\mathcal{O}$  as a function of  $H_f$  and  $t$ . Note that for observables commuting with  $H_i$  like energy the projection to the diagonal ensemble is not affecting the result, while for the observables which do not commute with  $H_i$  such projection makes a difference.

The expectation value of the observable  $\mathcal{O}$  is then

$$\langle \mathcal{O}(t) \rangle = \sum_n |\langle \psi(t) | n \rangle|^2 \langle n | \mathcal{O} | n \rangle = \sum_n p_n(t) \langle n | \mathcal{O} | n \rangle, \quad (24)$$

where  $|n\rangle$  denotes the energy eigenstates of  $H_i$  and  $p_n(t) = |\langle \psi(t) | n \rangle|^2$  are the probabilities of occupation of these states. Within a continuum description the sum above can be formally written as a continuous integral over energies

$$\langle \mathcal{O}(t) \rangle = \int dE P(E, t) \mathcal{O}(E, t), \quad (25)$$

where  $P(E, t) = \sum_n p_n(t) \delta(E - E_n)$  is the work distribution function for a double quench and

$$\mathcal{O}(E, t) = \sum_n \frac{p_n(t)}{P(E, t)} \langle n | \mathcal{O} | n \rangle \delta(E - E_n). \quad (26)$$

*Postselection.* The idea of postselection is that one can artificially skew the energy distribution  $P(E, t)$  by for example disregarding instances with energy above the certain threshold. From computational purposes it is more convenient, however, to skew the distribution by multiplying it by an exponential factor  $\exp(-\tilde{\beta}E)$ , where  $\tilde{\beta}$  plays the role of postselected temperature. We thus can formally define

$$P_{\tilde{\beta}}(E, t) = \frac{1}{\tilde{Z}_{\tilde{\beta}}(t)} P(E, t) e^{-\tilde{\beta}E}, \quad (27)$$

where  $\tilde{Z}_{\tilde{\beta}}(t)$  is the postselected partition function:

$$\tilde{Z}_{\tilde{\beta}}(t) = \int dE P(E, t) e^{-\tilde{\beta}E} = \sum_n p_{\tilde{\beta}, n}(t), \quad (28)$$

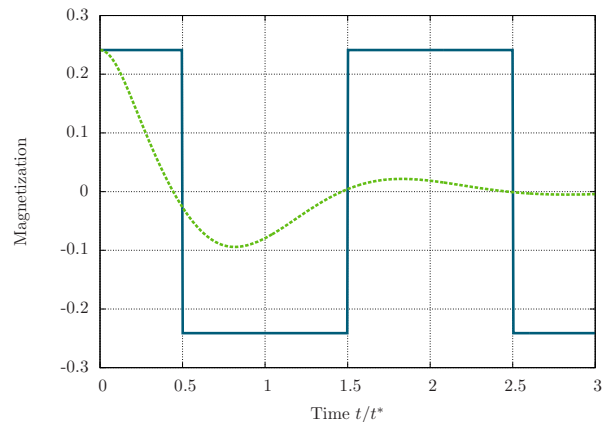


Figure 4: (Color online) Dynamics of the post-selected magnetization after a quench from  $g_i = 0.5$  to  $g_f = 1.5$ . While the blue (solid) curve shows the order parameter dynamics after a quench, the green (dashed) curve shows the zero-temperature limit  $\tilde{\beta} \rightarrow \infty$  of the post-selected magnetization.

with  $p_{\tilde{\beta}, n}(t) = p_n(t) \exp[-\tilde{\beta}E]$ . Then the post-selected expectation value of the observable will read:

$$\langle \mathcal{O}(t) \rangle_{\tilde{\beta}} = \sum_n p_{\tilde{\beta}, n} \langle n | \mathcal{O} | n \rangle. \quad (29)$$

yielding in the continuum description:

$$\langle \mathcal{O}(t) \rangle_{\tilde{\beta}} = \int dE \tilde{P}_{\tilde{\beta}}(E, t) \mathcal{O}_{\tilde{\beta}}(E, t). \quad (30)$$

We will not analyze in detail this postselection procedure here and its similarities and differences with thermodynamics (which is equivalent to preselection in our language) since this lies beyond the scope of our work. We only note that as the postselected temperature  $\tilde{T} = \tilde{\beta}^{-1}$  is lowered we are effectively projecting the observable to the ground state manifold. In Fig. 4 we show the postselected magnetization in this low temperature limit revealing jumps between the different symmetry broken sectors, which are located precisely at the Fisher times. Note that this allows one to observe real-time nonanalyticities in local observables. We anticipate that in this limit the magnetization dynamics will be decoherence free at the expense of effectively excluding large amounts of data from the analysis. This point will be a subject of our future work.

### Postselection and the complex time return amplitude

Let us make another brief point where postselection can be used to obtain nontrivial results. We now go back to a single quench of the Hamiltonian from  $H_i$  to  $H_f$ . Then as it was shown in Ref. [4] up to the phase factor the return amplitude  $G(t)$  is the Fourier transform of the

work distribution after the quench:

$$G(t) = \int dW P(W) \exp[iWt], \quad (31)$$

where

$$P(W) = \sum_n |\langle \psi_i | n^f \rangle|^2 \delta(E_n^f - E_0 - W), \quad (32)$$

where  $|n^f\rangle$  are the energy eigenstates of the final Hamiltonian and  $E_n^f$  are the corresponding eigenenergies.

Using similar considerations as in the previous section we can define the postselected work distribution function (but this time with respect to the eigenstates of the final Hamiltonian):

$$\tilde{P}_{\tilde{\beta}}(W) = \frac{1}{\tilde{Z}_{\tilde{\beta}}} P(W) \exp[-\tilde{\beta}W]. \quad (33)$$

Then trivially extending the analysis of Ref. [4] we find that the inverse Fourier transform of the postselected

work distribution function gives the return amplitude at a complex time:

$$\int dW \tilde{P}_{\tilde{\beta}}(W) \exp[iWt] = G(t + i\tilde{\beta}) \quad (34)$$

Thus amazingly the complex time return amplitude and hence the Fisher zeros analyzed in Fig. 1 of the main paper are measurable quantities at least in principle (note that the postselected temperature can be both positive and negative).

---

- [1] E. Barouch and B. McCoy, *Phys. Rev. A* **3**, 786 (1971).
- [2] M. Rigol, V. Dunjko and M. Olshanii, *Nature* **452**, 854 (2008).
- [3] A. Polkovnikov, K. Sengupta, A. Silva, and M. Vengalattore, *Rev. Mod. Phys.* **83**, 863 (2011).
- [4] A. Silva, *Phys. Rev. Lett.* **101**, 120603 (2008).